Forward diffraction dissociation of the virtual photons at small x_{Bj} in the QCD dipole picture

A.Bialas*and W.Czyz[†] M.Smoluchowski Institute of Physics Jagellonian University[‡]

December 2, 2018

Abstract

Forward differential cross-section for diffraction dissociation of virtual photons on nucleon target is calculated in the QCD dipole picture. The numerical estimates are presented and discussed.

PACS numbers: 12.38. Bx, 13.40. -f, 13.60. Hb

1 Introduction

It was shown recently [1, 2] that the QCD dipole picture [3, 4, 5] can successfully describe the HERA data [6] on proton structure function F_2 at small $x_{\rm Bj}$ in a wide range of Q^2 . This important observation, indicating that the BFKL dynamics [7] may be relevant already in the kinematic region accessible at the existing machine, invites one to apply the same methods for description of other related processes. The problem is particularly interesting in view of the conflicting opinions about the subject [8].

^{*}e-mail:bialas@thp1.if.uj.edu.pl

[†]e-mail:czyz@thp1.if.uj.edu.pl

[‡]Address: 30-059 Krakow, Reymonta 4

Diffraction dissociation of the virtual photons, also measured recently at HERA [9], presents a challenging example of such a process. Indeed, if one takes the traditional point of view [10] that both elastic and inelastic diffractive amplitudes at high energies are consequences of absorption of the incident particle waves, it follows that the total cross-section (related to forward elastic amplitude by the optical theorem) and the forward diffraction cross-section should be very closely related. In the present paper we explore this relation in the framework of the QCD dipole picture.

There are several reasons for a particular interest in studying of the *forward* diffraction dissociation in the QCD dipole picture.

- First, as we show below, the theoretical calculation does not introduce new parameters as compared to those already known from the fit to the total cross-section measurements [1, 2]. Some minor ambiguities which appear in the final result are related to the limits of the validity of the model itself and thus may serve as important clues for the extension of the whole picture.
- Second, the relation between the total cross-section and diffraction dissociation being quadratic, their comparison provides a sensitive test of the model, in particular of the absolute normalization of the cross-sections, difficult to obtain by any other method. In view of the possibility that measurements of the forward diffraction dissociation may be soon available [11], our exercise can also be of some practical importance.
- Third, the BFKL dynamics implies that the behaviour of the forward amplitudes cannot be obtained by a simple extrapolation of the high-energy limit found at finite momentum transfer [4, 12]. It is thus interesting to investigate separately the point $p_t = 0$.
- Fourth, forward diffraction dissociation is the process which dominates the shadowing of virtual photons in nuclei. It is therefore important to know it as well as possible if one wants to study the multiple scattering effects.
- Finally, the calculation at $p_t = 0$ is technically simpler than that in the general case of arbitrary momentum transfer. This permits to have a much better control of the underlying assumptions and of the restrictions implied by the limited validity of the QCD dipole picture.

Recently, using the QCD dipole picture, we have derived the formulae for nuclear shadowing of high-energy virtual photons [13]. As noted above, this process is closely related to the diffractive phenomena. We shall explore this relation in the present paper.

Diffraction dissociation in the framework of the BFKL dynamics was already discussed extensively [12, 15] using the momentum representation of the amplitudes. Our approach, based on the QCD dipole technique [3, 4, 5], is closer to that of [18, 19] where the impact parameter representation is used instead.

In the next section we explain the meaning of the two components of diffractive dissociation, as defined in [16, 17]. Section 3 and 4 present the major result of this paper, i.e. the calculation of the diffractive structure functions at $p_t = 0$. Saddle point approximation is discussed in Section 5 and numerical results in Section 6. Our conclusions are listed in the last section.

2 Two components of the diffractive crosssection

As was observed in [16, 17] (cf. also [12, 19]), the cross-section for diffraction dissociation in the QCD dipole model can be written as a sum of the two components

(i) Quasi-elastic component, arising from the elastic scattering of the $q\bar{q}$ pair emerging from the virtual photon. This component may be considered as a generalization of the Vector Dominance Model [20, 21]: The sum over masses of vector mesons is replaced by integral over the masses of the $q\bar{q}$ pair. Also the transitions between the states with different relative transverse momenta of q and \bar{q} (i.e. of different masses of the system) are taken explicitly into account. Of course, such an approximation can be reasonable only in the continuum part of the system, outside the prominent vector meson resonances. For the explicit calculations of the exclusive vector meson production, see [22] and [23].

The quasi-elastic component contributes mostly to diffractive excitation of the masses of the order of Q^2 , more precisely in the region $\beta \geq .1$ where,

as usual,

$$\beta = \frac{Q^2}{Q^2 + M^2} \,, \tag{1}$$

and M is the mass of the diffractively produced system.

(ii) Direct component, corresponding to the direct (two gluon exchange) interaction of the full dipole cascade developed from the primary fluctuation of the virtual photon. This component can be regarded as a realization of the so-called triple-pomeron coupling [24] in the QCD dipole picture [4]. It contributes mainly to the region of very large masses, $\beta \ll 1$.

3 Quasi-elastic component

As is clear from its definition, the amplitude for the quasi-elastic scattering of a virtual photon on a dipole of the transverse diameter r_0 , leading to a final state consisting of quark and antiquark of the total mass M and the relative transverse momentum \vec{k} , can be written as

$$\langle \vec{k}, M^2 \mid T^{\text{qel}} \mid Q \rangle$$

$$= \int_0^1 d\eta \int d^2r \langle \vec{k}, M^2 \mid \vec{r}, \eta \rangle \langle \vec{r}, \eta \mid T \mid \vec{r}, \eta \rangle \Psi(\vec{r}, \eta; Q) , \qquad (2)$$

where $\Psi(\vec{r}, \eta; Q)$ are the light-cone photon wave functions [25], with \vec{r} being the quark-antiquark relative transverse distance and η the light-cone momentum function of one of the quarks,

$$\langle \vec{r}, \eta \mid T \mid \vec{r}, \eta \rangle \equiv T(r, r_0; Y) = \pi \alpha^2 r_0^2 \int \frac{d\gamma}{2\pi i} e^{\Delta(\gamma)Y} \left(\frac{r}{r_0}\right)^{\gamma} h(\gamma)$$
 (3)

is the forward dipole-dipole elastic amplitude in the QCD dipole picture with [5, 13, 14]

$$h(\gamma) = \frac{4}{\gamma^2 (2 - \gamma)^2} \tag{4}$$

and

$$\Delta(\gamma) = \frac{\alpha N}{\pi} \left[2\psi(1) - \psi\left(1 - \frac{\gamma}{2}\right) - \psi\left(\frac{\gamma}{2}\right) \right], \tag{5}$$

 α being the strong coupling constant. Following [1] we take $Y = \log(c/x_{\rm Bj})$, where c is a constant.

Using the argument given in [17], the cross-section for scattering on the nucleon target can be expressed in the form

$$\frac{d\sigma^{\text{qel}}(p_t = 0)}{dM^2 d^2 p_t} = \frac{2N_c n_{\text{eff}}^2}{4\pi^2} \int d^2 k \mid \langle \vec{k}, M^2 \mid T^{\text{qel}} \mid Q \rangle \mid^2$$

$$= \frac{2N_c n_{\text{eff}}^2}{4\pi^2} \int_0^1 d\eta \eta (1 - \eta) \frac{d\phi_k}{2} \mid G(r_0, \vec{k}(\hat{M}), \eta, Y; Q) \mid^2, (6)$$

where

$$G(r_0, \vec{k}, \eta, Y; Q) = \frac{1}{2\pi} \int d^2r e^{i\vec{k}\vec{r}} T(r, r_0, Y) \Psi(\vec{r}, \eta; Q) . \tag{7}$$

The two-dimensional vector $\vec{k}(\hat{M})$ points in the direction of \vec{k} (described by the azimuthal angle ϕ_k) and its length equals

$$|\vec{k}(\hat{M})| = \hat{M} \equiv M(\eta(1-\eta))^{\frac{1}{2}}.$$
 (8)

The factor 2 in the first equality of (6) takes care of the sum over different spin configurations of the $q\bar{q}$ pair ¹, N_c results from the sum over colours, and n_{eff}^2 takes care of the average number of dipoles in a nucleon [1]. It is not difficult to verify that after integrating over dM^2 , Eq. (6) gives the familiar formula for the integrated diffractive cross-section [10]

$$\frac{d\sigma^{\text{qel}}}{d^2 p_t} = \frac{2N_c n_{\text{eff}}^2}{4\pi^2} \int_0^1 d\eta \int d^2 r \mid \langle \vec{r}, \eta \mid T^{\text{qel}} \mid \vec{r}, \eta \rangle \mid^2 \mid \Psi(\vec{r}, \eta; Q) \mid^2.$$
 (9)

Using the formulae for $\Psi(r, \eta; Q)$ [25]

$$\Psi_{T,\text{right}}(r,\eta;Q) = \frac{\sqrt{\alpha_{\text{em}}}e_{(f)}}{2\pi}\eta \hat{Q}e^{i\phi_r}K_1(\hat{Q}r), \qquad (10)$$

$$\Psi_{T,\text{left}}(r,\eta;Q) = \frac{\sqrt{\alpha_{\text{em}}}e_{(f)}}{2\pi}(1-\eta)\hat{Q}e^{-i\phi_r}K_1(\hat{Q}r), \qquad (11)$$

$$\Psi_L(r,\eta;Q) = \frac{\sqrt{\alpha_{\rm em}}e_{(f)}}{2\pi}2\eta(1-\eta)QK_0(\hat{Q}r),$$
 (12)

¹This factor was missing in [17].

where $\alpha_{\rm em}$ is the electromagnetic coupling constant and $e_{(f)}$ the charge of the quark of flavour f, one can integrate over the azimuthal angle in (7). One obtains

$$G_{T,\text{right}}(\eta, k; Y; Q) = \frac{\sqrt{\alpha_{\text{em}}} e_{(f)}}{2\pi} \eta \hat{Q} \int r dr T(r, r_0; Y) K_1(\hat{Q}r) J_1(\hat{M}r) , \quad (13)$$

$$G_L(\eta, k; Y; Q) = \frac{\sqrt{\alpha_{\text{em}}} e_{(f)}}{2\pi} 2\eta (1 - \eta) Q \int r dr T(r, r_0; Y) K_0(\hat{Q}r) J_0(\hat{M}r) , \quad (14)$$

 $G_{T,\text{left}}(\eta, k; Y; Q)$ is obtained from $G_{T,\text{right}}(\eta, k; Y; Q)$ by substitution $\eta \to 1 - \eta$. The integrals over dr can be found in [26] and we finally obtain

$$G_{T,\text{right}}(\eta, M; Y; Q) = \frac{\sqrt{\alpha_{\text{em}}} e_{(f)} \alpha^2}{2} r_0^2 \eta \hat{Q}^{-1} \frac{M}{Q} \int_{c-i\infty}^{c+i\infty} \frac{d\lambda}{2\pi i} e^{\Delta(\lambda)Y}$$

$$\times \left(\frac{2}{\hat{Q}r_0}\right)^{\lambda} H_T(\lambda) F\left(2 + \frac{\lambda}{2}, 1 + \frac{\lambda}{2}; 2; -\frac{M^2}{Q^2}\right), \tag{15}$$

$$G_L(\eta, M; Y; Q) = \sqrt{\alpha_{\rm em}} e_{(f)} \alpha^2 r_0^2 Q^{-1} \int_{c-i\infty}^{c+i\infty} \frac{d\lambda}{2\pi i} e^{\Delta(\lambda)Y}$$

$$\times \left(\frac{2}{\hat{Q}r_0}\right)^{\lambda} H_L(\lambda) F\left(1 + \frac{\lambda}{2}, 1 + \frac{\lambda}{2}; 1; -\frac{M^2}{Q^2}\right), \tag{16}$$

where

$$H_L(\lambda) = \Gamma^2(1 + \frac{\lambda}{2})h(\lambda), \quad H_T(\lambda) = (1 + \frac{\lambda}{2})H_L(\lambda)$$
 (17)

and F(a, b, c, z) is the hypergeometric function.

The next step is to introduce (15), (16) into (6) and perform the integration over $d\eta$ (integration over $d\phi_k$ gives 2π because the integrand does not depend on ϕ_k). Using the relation

$$\frac{dF}{d^2 p_t} = \frac{Q^2}{4\pi^2 \alpha_{\rm em}} x_P^{-1} \frac{d\sigma}{dy d^2 p_t} = \frac{Q^4}{4\pi^2 \alpha_{\rm em}} x^{-1} \frac{d\sigma}{dM^2 d^2 p_t}$$
(18)

with $x_P = x_{\rm Bi}/\beta$, we finally obtain for the structure functions

$$\frac{dF_T^{\text{qel}}}{d^2 p_t}(Q^2, x_P, \beta, p_t = 0) = \frac{e_f^2 \alpha^4 N_c}{16\pi^3} n_{\text{eff}}^2 \frac{Q^2 r_0^4}{x_P}$$

$$\times (1 - \beta) \int_{c - i\infty}^{c + i\infty} \frac{d\lambda_1}{2\pi i} e^{\Delta(\lambda_1)Y} H_T(\lambda_1) \left(\frac{2\sqrt{\beta}}{Qr_0}\right)^{\lambda_1} F(1 + \frac{\lambda_1}{2}, -\frac{\lambda_1}{2}; 2; 1 - \beta)
\times \int_{c - i\infty}^{c + i\infty} \frac{d\lambda_2}{2\pi i} e^{\Delta(\lambda_2)Y} H_T(\lambda_2) \left(\frac{2\sqrt{\beta}}{Qr_0}\right)^{\lambda_2} F(1 + \frac{\lambda_2}{2}, -\frac{\lambda_2}{2}; 2; 1 - \beta) K_T(\lambda),$$
(19)

$$\frac{dF_L^{\text{qel}}}{d^2 p_t} (Q^2, x_P, \beta, p_t = 0) = \frac{e_f^2 \alpha^4 N_c}{8\pi^3} n_{\text{eff}}^2 \frac{Q^2 r_0^4}{x_P}
\times \beta \int_{c-i\infty}^{c+i\infty} \frac{d\lambda_1}{2\pi i} e^{\Delta(\lambda_1)Y} H_L(\lambda_1) \left(\frac{2\sqrt{\beta}}{Qr_0}\right)^{\lambda_1} F(1 + \frac{\lambda_1}{2}, -\frac{\lambda_1}{2}; 1; 1 - \beta)
\times \int_{c-i\infty}^{c+i\infty} \frac{d\lambda_2}{2\pi i} e^{\Delta(\lambda_2)Y} H_L(\lambda_2) \left(\frac{2\sqrt{\beta}}{Qr_0}\right)^{\lambda_2} F(1 + \frac{\lambda_2}{2}, -\frac{\lambda_2}{2}; 1; 1 - \beta) K_L(\lambda),$$
(20)

where $\lambda = \lambda_1 + \lambda_2$ and

$$K_L(\lambda) = \frac{\Gamma^2(2 - \frac{\lambda}{2})}{\Gamma(4 - \lambda)}, \quad K_T(\lambda) = \frac{2 - \frac{\lambda}{2}}{1 - \frac{\lambda}{2}} K_L(\lambda). \tag{21}$$

 e_f^2 is the sum of squares of the quark charges.

The hypergeometric functions from (15), (16) were transformed into those in (19), (20) using the relation [27]

$$F(b+n,b;n+1;1-\frac{1}{\beta}) = \beta^b F(b,1-b;1+n;1-\beta), \qquad (22)$$

where n = 0 for longitudinal and n = 1 for the transverse component.

4 Direct (3-Pomeron) component

Cross-section for the direct component can be written as

$$\frac{d\sigma^{\text{dir}}}{dyd^{2}p_{t}} = n_{\text{eff}}^{2} \int_{0}^{1} d\eta \int d^{2}r |\Psi(r,\eta;Q)|^{2} \frac{\sigma_{d}(r,r_{0},Y,y;p_{t})}{dyd^{2}p_{t}}, \qquad (23)$$

where $\sigma_d(r, r_0, Y, y)$ is the cross-section for diffractive dissociation of the dipole of transverse diameter r, scattering off the dipole of transverse diameter r_0 , with $Y - y = -\log \beta$.

The formula for $\sigma_d(r, r_0, Y, y; p_t)$ at $p_t = 0$ can be derived using the Mueller-Patel formulation [4]. We have

$$\frac{\sigma_d(r, r_0, Y, y; p_t = 0)}{dy d^2 p_t} = \frac{1}{4\pi^2} \int \frac{dx_1}{x_1} \frac{dx_2}{x_2} \frac{dx_1'}{x_1'} \frac{dx_2'}{x_2'} \times \tau(x_1, x_1') \tau(x_2, x_2') \rho_1(r_0, x_1, y^*) \rho_1(r_0, x_2, y^*) \rho_2(r, x_1', x_2'; Y - y^*, y - y^*),$$
(24)

where $\rho_1(r_0, x, y^*)$ is the single dipole density in the dipole of the transverse diameter r_0 given by

$$\rho_1(r_0, x, y^*) = \int_{c-i\infty}^{c+i\infty} \frac{d\lambda}{2\pi i} e^{\Delta(\lambda)y^*} \left(\frac{r_0}{x}\right)^{\lambda}, \qquad (25)$$

 $\tau(x, x')$ is the forward scattering amplitude for collision of two dipoles of transverse diameters x and x' (given in [4]), and $\rho_2(r, x'_1, x'_2; Y - y^*, y - y^*)$ is the two-dipole density in an dipole of transverse diameter r. The equation for $\rho_2(r, x'_1, x'_2; Y, y)$ was written down in [4]. It reads

$$\rho_{2}(r, x'_{1}, x'_{2}; Y, y)
= \frac{\alpha N_{c}}{\pi^{2}} \Theta(Y - y) \int \frac{x_{01}^{2} d^{2} x_{2}}{x_{02}^{2} x_{12}^{2}} e^{-(Y - y)\Omega} \rho_{1}(x_{02}, x'_{1}, y) \rho_{1}(x_{12}, x'_{2}, y)
+ \frac{\alpha N_{c}}{\pi^{2}} \int \frac{x_{01}^{2} d^{2} x_{2}}{x_{02}^{2} x_{12}^{2}} \int_{y}^{Y} dy' e^{-(Y - y')\Omega} \rho_{2}(x_{02}, x'_{1}, x'_{2}; y', y), \qquad (26)$$

where Ω is the ultraviolet cut-off defined in [4] (the final result does not depend on Ω). Eq. (26) shows clearly the physical meaning of $\rho_2(r, x'_1, x'_2; Y, y)$: the first term describes emission of a single gluon at rapidity y followed by independent evolution of two dipoles (formed from the produced gluon and the original $q\bar{q}$ pair), each producing ρ_1 new dipoles; The second term describes the evolution of the original dipole from rapidity Y until y.

It is important to realize that the Eq. (26) can be trusted only if y is not too close to Y. Indeed, the basic assumption of the BFKL approximation is

that the longitudinal momenta of emitted gluons are strongly ordered, i.e. the momentum of each emitted gluon is much smaller than that of the previous one. In the case we consider, the point y = Y corresponds to the first emitted gluon taking all momentum of the initial quarks. This is of course in blatant contradiction to the very idea of the BFKL physics. The problem can be cured by introducing an appropriate cut-off which would eliminate such unphysical configurations. Unfortunately, there is no unique way to do it and thus the result is ambiguous. In order to obtain an idea about the scale of this uncertainty, we have considered a modified equation for $\rho_2(r, x'_1, x'_2; Y, y)$ in which we replaced the function $\Theta(Y - y)$ in the first term on the RHS of (26) by a function $\omega(Y - y)$ representing the required cut-off in longitudinal momentum of the emitted gluon. We have then studied the results varying the cut-off. They are described in Section 6.

Following closely the method shown in [13], Eq. (26) can be solved with the result

$$\rho_2(r, x_1', x_2'; Y, y) = \frac{\alpha N_c}{\pi^2} \int_{c-i\infty}^{c+i\infty} \frac{d\lambda}{2\pi i} r^{\lambda} e^{\Delta(\lambda)(Y-y)} \int_0^{\infty} dx_{01} x_{01}^{-1-\lambda} \times \int \frac{x_{01}^2 d^2 x_2}{x_{02}^2 x_{12}^2} \rho_1(x_{02}, x_1', y) \rho_1(x_{12}, x_2', y) \theta(\lambda, Y, y) , \qquad (27)$$

where

$$\theta(\lambda, Y, y) = \int_{-y}^{Y-y} e^{-\Delta(\lambda)u} \frac{d\omega(u)}{du} du.$$
 (28)

For $\omega(u) \equiv \Theta(u)$ (as in (26)), $\theta(\lambda, Y, y)$ reduces trivially to $\Theta(Y - y)$.

When (27) is introduced into (24) the integrals can be explicitly performed and the final result is [13]

$$\frac{\sigma_d(r, r_0, Y, y; p_t = 0)}{dy d^2 p_t} = \frac{\alpha^5 N_c}{4\pi} r_0^4 \int_{c-i\infty}^{c+i\infty} \frac{d\lambda_1}{2\pi i} e^{\Delta(\lambda_1)y} h(\lambda_1) G(\lambda_1)
\times \int_{c-i\infty}^{c+i\infty} \frac{d\lambda_2}{2\pi i} e^{\Delta(\lambda_2)y} h(\lambda_2) G(\lambda_2) e^{\Delta(\lambda)(Y-y)} \left(\frac{r}{r_0}\right)^{\lambda} \frac{\theta(\lambda, Y, y)}{G(\lambda)},$$
(29)

where
$$\lambda = \lambda_1 + \lambda_2$$
 and $G(\lambda) = \frac{\Gamma(\lambda/2)}{\Gamma(1-\lambda/2)}$.

Averaging over the photon wave functions can also be explicitly performed and one finally obtains

$$\frac{d\sigma_{T,L}^{\text{dir}}(p_t=0)}{dyd^2p_t} = n_{\text{eff}}^2 \sigma_{T,L}^*(Q, r_0, Y, y; p_t=0),$$
(30)

where $\sigma_{T,L}^*$ is given by (29) with the substitution

$$r^{\lambda} \to \frac{N_c \alpha_{\text{elm}} e_f^2}{\pi} \left(\frac{2}{Q}\right)^{\lambda} I_{T,L}(\lambda)$$
 (31)

with

$$I_L(\lambda) = 2 \frac{\Gamma^2(2 - \frac{\lambda}{2})\Gamma^4(1 + \frac{\lambda}{2})}{\Gamma(2 + \lambda)\Gamma(4 - \lambda)}, \quad I_T(\lambda) = \frac{(2 - \frac{\lambda}{2})(1 + \frac{\lambda}{2})}{\lambda(1 - \frac{\lambda}{2})} I_L(\lambda).$$
 (32)

The indices T, L refer to the transverse and longitudinal photons, respectively.

Using the relation (18) we can thus write for the diffractive structure function

$$\frac{dF_{T,L}^{\text{dir}}}{d^2 p_t}(Q^2, x_P, \beta, p_t = 0) = \frac{\alpha^5 N_c^2 e_f^2}{16\pi^4} n_{\text{eff}}^2 \frac{Q^2 r_0^4}{x_P} \int_{-i\infty}^{c+i\infty} \frac{d\lambda_1}{2\pi i} e^{\Delta(\lambda_1)y} h(\lambda_1) G(\lambda_1)$$

$$\times \int_{c-i\infty}^{c+i\infty} \frac{d\lambda_2}{2\pi i} e^{\Delta(\lambda_2)y} h(\lambda_2) G(\lambda_2) e^{\Delta(\lambda)(Y-y)} \left(\frac{2}{Qr_0}\right)^{\lambda} \frac{I_{T,L}(\lambda)}{G(\lambda)} \theta(\lambda, Y, y) . \quad (33)$$

5 Saddle-point approximation

Before discussing the numerical results, it is interesting to consider the saddlepoint approximation which gives the limiting behaviour of structure functions when $x_P \to 0$.

For $F_L^{\rm qel}$ the calculation is straightforward, we simply evaluate independently the two integrals. The position of the saddle point (identical for λ_1 and for λ_2) is

$$\lambda_c = 1 + a(Y) \log \left(\frac{Qr_0}{2\sqrt{\beta}} \right) > 1, \qquad (34)$$

where

$$a(Y) = \frac{1}{\Delta''(1)Y} = \frac{\pi}{7\alpha N_c \zeta(3)Y} \tag{35}$$

so that we obtain

$$\frac{dF_L^{\text{qel}}}{d^2 p_t} = \frac{e_f^2 \alpha^4 N_c}{8\pi} r_0^2 n_{\text{eff}}^2 c^{2\Delta_P} x_P^{-1-2\Delta_P} \frac{2a(Y)}{\pi} \times \beta^{2-2\Delta_P} F^2(3/2, -1/2; 1; 1-\beta) \exp\left(-a(Y) \log^2\left(\frac{Qr_0}{2\sqrt{\beta}}\right)\right) . \quad (36)$$

We see from (36) that $F_L^{\rm qel}$ shows a typical BFKL power-law behaviour in x_P (modified by logarithmic corrections, similarly as in case of $F_2(Q^2, x_{\rm Bj})$ [1, 29]). The β dependence is also dominated by the power-law modified by a hypergeometric function. The scaling is violated by the last factor which decreases with increasing Q^2 and mixes in a complicated way the $Q-,\beta-$ and the energy dependence.

In the case of F_T^{qel} the simple procedure used above fails because the integrand has a pole at $\lambda_1 + \lambda_2 = 2$ and thus the contour of integration can be moved to the position of saddle point only after the contribution from the pole is added. To obtain this contribution we first move the contour in λ_2 complex plane to the right of the point $2 - \lambda_1$. The contribution from the pole is then easily found to be

$$\frac{dF_T^{\text{qel}}}{d^2 p_t}_{pole} = \frac{e_f^2 \alpha^4 N_c}{2\pi^3} r_0^2 n_{\text{eff}}^2 x_P^{-1} \beta (1 - \beta) \int_{c-i\infty}^{c+i\infty} \frac{d\lambda}{2\pi i} e^{2\Delta(\lambda)Y} H_T(\lambda) H_T(2 - \lambda) \times F(1 + \lambda/2, -\lambda/2; 2; 1 - \beta) F(2 - \lambda/2, \lambda/2 - 1; 2; 1 - \beta).$$
(37)

The integral over $d\lambda$ can now be evaluated by the saddle-point method and we obtain

$$\frac{dF_T^{\text{qel}}}{d^2 p_t}_{pole} = \frac{9e_f^2 \alpha^4 N_c}{16\pi} r_0^2 n_{\text{eff}}^2 c^{2\Delta_P} x_P^{-1-2\Delta_P} \left(\frac{2a(2Y)}{\pi}\right)^{\frac{1}{2}} \times \beta^{1-2\Delta_P} (1-\beta) F^2(3/2, -1/2; 2; 1-\beta).$$
(38)

One should add to this the integral to the right of the pole. This integral can be estimated by the saddle point method because now the contours are to the right of 1 (in both complex planes). The resulting contribution is

$$\Delta \left(\frac{dF_T^{\text{qel}}}{d^2 p_t} \right) = -\frac{9e_f^2 \alpha^4 N_c}{32\pi^2} r_0^2 n_{\text{eff}}^2 c^{2\Delta_P} x_P^{-1-2\Delta_P} \beta^{1-2\Delta_P} (1-\beta)
\times F^2(3/2, -1/2; 2; 1-\beta) \left(\frac{1}{\log(Qr_0/2\sqrt{\beta})} \right) \exp\left(-a(Y)log^2 \left(\frac{Qr_0}{2\sqrt{\beta}} \right) \right).$$
(39)

The interesting feature is that while the pole contribution scales exactly, the remaining integral increases with Q^2 (it decreases in absolute value but has a negative sign). Consequently, $F_T^{\rm qel}$ increases with increasing Q^2 . Otherwise the behaviour is qualitatively similar to that of $F_L^{\rm qel}$ except for the "kinematical" factor $M^2/Q^2 = (1-\beta)/\beta$ (implying that the transverse component dominates over the longitudinal one everywhere except in the vicinity of $\beta = 1$).

For $F_2^{\text{qel}} = F_T^{\text{qel}} + F_L^{\text{qel}}$ we thus obtain a fairly complicated Q^2 dependence reflecting β -dependent mixing of the transverse and longitudinal contributions.

Direct component can be approximated by first performing the saddle point in $\omega \equiv (\lambda_1 - \lambda_2)/2$ and then in λ . We only give here results without the cut-off, i.e. for $\theta(\lambda, Y, y) \equiv \Theta(Y - y)$.

After first integration ($\omega_{\text{saddle}} = 0$) we obtain

$$\frac{dF_{T,L}^{\text{dir}}}{d^2 p_t} = \frac{\alpha^5 N_c^2 e_f^2}{16\pi^4} n_{\text{eff}}^2 \frac{Q^2 r_0^4}{x_P} \frac{1}{2\pi} \int_{-i\infty}^{+i\infty} \frac{d\lambda}{2\pi i} \frac{\sqrt{\pi}}{\sqrt{\Delta''(\lambda/2)y}} e^{2\Delta(\lambda/2)y}
\times h^2(\frac{\lambda}{2}) G^2(\frac{\lambda}{2}) e^{\Delta(\lambda)(Y-y)} \left(\frac{2}{Qr_0}\right)^{\lambda} \frac{I_{T,L}(\lambda)}{G(\lambda)}.$$
(40)

The integral over λ is somewhat more complicated. The saddle point equation is

$$\Delta'(\lambda_c/2)y + \Delta'(\lambda_c)(Y - y) = \log(Qr_0/2). \tag{41}$$

This can be solved in two steps. First we find λ_0 from the equation

$$\Delta'(\lambda_0/2)y + \Delta'(\lambda_0)(Y - y) = 0.$$
(42)

Then we write $\lambda_c = \lambda_0 + \delta$. δ can be found from (41):

$$\delta = \tilde{a}(Y - y, y) \log(Qr_0/2), \qquad (43)$$

where

$$\tilde{a}(Y - y, y) = \frac{1}{\Delta''(\lambda_0)(Y - y) + \frac{1}{2}\Delta''(\lambda_0/2)y},$$
(44)

 $\delta \to 0$ in the limit $y \gg 1$, $(Y - y) \gg 1$, so that the approximation is correct. When this is introduced into (40) we obtain

$$\frac{dF_{T,L}^{\text{dir}}}{d^{2}p_{t}} = \frac{\alpha^{5}N_{c}^{2}e_{f}^{2}}{64\pi^{4}}n_{\text{eff}}^{2}\frac{Q^{2}r_{0}^{4}}{x_{P}}\left(\frac{2\tilde{a}(0,y)}{\pi}\right)^{\frac{1}{2}}e^{2\Delta(\lambda_{0}/2)y}
\times h^{2}(\frac{\lambda_{0}}{2})G^{2}(\frac{\lambda_{0}}{2})e^{\Delta(\lambda_{0})(Y-y)}\left(\frac{2}{Qr_{0}}\right)^{\lambda_{0}}\frac{I_{T,L}(\lambda_{0})}{G(\lambda_{0})}
\times \left(\frac{2\tilde{a}(Y-y,y)}{\pi}\right)^{\frac{1}{2}}\exp\left(-\frac{1}{2}\tilde{a}(Y-y,y)\log^{2}(Qr_{0}/2)\right).$$
(45)

Unfortunately, this requires solution of the Eq. (42) and thus numerical work.

The major new effect seen from (45) is that here the x_P and β dependence are no longer determined by the BFKL pomeron intercept². Instead, the relevant powers depend on λ_0 which, in turn, is a function of the ratio y/Y. Thus a rather complicated structure appears. In figure $1 \Delta(\lambda_0/2)$ and $\Delta(\lambda_0)$ which determine the powers in x_P and β dependence are shown. One sees that they are always larger than Δ_P . Another interesting observation is that the dominant factor in Q dependence is $Q^{2-\lambda_0}$ instead of Q found in $F_2(Q^2, x_{\text{Bj}})$ [3, 4, 1]. One sees in Fig. 1 that $2 - \lambda_0$ is substantially smaller than one and thus the effect is significant.

6 Numerical estimates

We have performed numerical estimates of the results presented in previous sections using the parameters given in [1].

In Figure 2 the β dependence of longitudinal and transverse photon contributions to the quasi-elastic component of the structure function is shown. One sees that the quasi-elastic transverse contribution largely dominates the longitudinal one, except at $\beta \approx 1$ where the longitudinal one fills the dip.

Such a large value of the quasi-elastic transverse component can be traced to the presence of the pole at $\lambda_1 + \lambda_2 = 2$ in the integrand of (19) which

²This effect was already discussed in [12, 15].

Figure 1: x_P and β dependences of the asymptotic formula for triple pomeron contribution to $\frac{dF_2}{d^2p_t}(p_t=0)$. The ratios of powers of x_P and β are potted versus $\frac{y}{Y-y}$. λ_0 is the approximate position of the saddle point. See text for details.

gives the main contribution to the integral. This pole, in turn, arises from integration over the regions of η close to zero and one, where the cut-off on the transverse size of the photon (as expressed by the Mc Donald function in (10), (11)) is ineffective. We thus see that an important contribution to the transverse quasi-elastic component comes from the non-perturbative region of large transverse sizes of the photon³. To investigate this problem in more detail, we have calculated the structure functions under the condition that the cutoff in photon size should never be larger than a certain parameter R, i.e.

$$\eta(1-\eta)Q^2 \ge \frac{1}{R^2} \,. \tag{46}$$

The resulting formulae are identical to Eqs. (19), (20) and (33) where now

³Numerous authors pointed out this effect, see e.g. [28]. The problem was also noted in [16, 17] where the integration over the photon size was restricted to a finite region $r \le r_0$.

Figure 2: β - dependence of the longitudinal and transverse photon contribution to the quasi-elastic component of the structure function $\frac{dF^{\rm qel}}{d^2p_t}(p_t=0)$. Solid lines - no cutoff. Broken lines - a cutoff for the non-perturbative region of large transverse sizes of the photon is introduced. For more details see the text.

$$K_{L}(\lambda) \to \tilde{K}_{L}(\lambda) \equiv \int_{\epsilon}^{1-\epsilon} d\eta [\eta(1-\eta)]^{1-\frac{\lambda}{2}},$$

$$K_{T}(\lambda) \to \tilde{K}_{T}(\lambda) \equiv \int_{\epsilon}^{1-\epsilon} d\eta \eta^{2} [\eta(1-\eta)]^{-\frac{\lambda}{2}},$$

$$I_{L}(\lambda) \to \tilde{I}_{L}(\lambda) \equiv 2\frac{\Gamma^{4}(1+\frac{\lambda}{2})}{\Gamma(2+\lambda)}\tilde{K}_{L}(\lambda),$$

$$I_{T}(\lambda) \to \tilde{I}_{T}(\lambda) \equiv 2\frac{2+\lambda}{\lambda} \frac{\Gamma^{4}(1+\frac{\lambda}{2})}{\Gamma(2+\lambda)}\tilde{K}_{T}(\lambda),$$

$$(47)$$

where

$$\epsilon = \frac{1}{2} \left(1 - \sqrt{1 - \frac{4}{R^2 Q^2}} \right) \approx \frac{1}{R^2 Q^2}.$$
(48)

The sensitivity to this "non-perturbative" contribution can be seen from Figure 2 where the β dependence following from (46,47) for $R=r_0$ is also plotted. One sees that $F_T^{\rm qel}$ is reduced by a factor of about 2, in comparison with the uncut result, whereas the longitudinal component is hardly affected. We thus conclude that the QCD dipole picture does not provide a reliable prediction for $F_T^{\rm qel}$: it must be supplemented by an additional non-perturbative input. Inverting this argument, one may say that measurements of this component can give interesting information on non-perturbative structure in the small $x_{\rm Bj}$ region.

The Q-dependence of the quasi-elastic component is shown in Figs. 3a and 3b. One sees that indeed, as was seen qualitatively from the saddle-point approximation, the longitudinal component decreases whereas the transverse one increases with increasing Q. In result F_2^{qel} decreases at $\beta = 1$, is almost constant at $\beta \approx 0.8$, and increases at smaller β . The comparison between figures 4a and 4b shows that this qualitative behaviour is unaffected by the cut (46), although the precise rate of change of course depends on it.

We have also calculated the x_P dependence. It shows a simple power law behaviour, consistent with the expectations from the saddle-point formulae of Section 5.

The β -dependence of the 3-Pomeron component is plotted in figure 4 in the log-log scale. As described in Section 4, we have investigated the dependence of the results on the cutoff in the rapidity of the emitted gluons. The cutoff function was taken in the form

$$\omega(Y - y) = \left(1 - e^{y - Y}\right)^k,\tag{49}$$

where k is a constant.

The results in Fig.4 are shown for k = 0 (no cut), k = 1 and k = 2. One sees that the uncut distribution follows very closely a power law, $\beta^{-.34}$, in the full region of β . This power is significantly larger than Δ_P , as expected from the discussion in Section 5. The effects of the cutoff (49) is twofold. First, as expected, it reduces strongly the structure function at large β (at $\beta = 1$ the structure function vanishes) and thus changes its shape. The structure function is affected, however, also in the region of small β , $\beta \leq .1$, where it is simply multiplied by a constant (smaller than one).

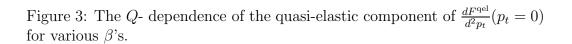


Figure 4: The triple-pomeron contribution to $\frac{dF_2}{d^2p_t}(p_t=0)$ for various cutoff's given by Eq. (49) and discussed in the text.

We thus see that without a better understanding of the energy-momentum conservation constraints in gluon emission (which are responsible for the cutoff in the gluon rapidity spectrum) there is little hope to obtain accurate predictions for the 3-pomeron component of the structure function, even in the region of small β .

Recently, Andersson [32] suggested that the energy-momentum conservation constraints in gluon emission can be taken into account by simply cutting out $\frac{11}{6}$ from the edge of the available phase-space in rapidity.⁴ The result of this prescription (which amounts to take $\omega(Y-y) \equiv \Theta(Y-y-\frac{11}{6})$ and thus simply changes β into $\beta e^{-11/6} \approx .16\beta$) is also shown in Fig.4. One sees that the value of the 3-pomeron component in the small β region is reduced by a factor of about 2.

7 Conclusions and outlook

Using the QCD dipole picture, we have derived the formulae for the forward cross-section of diffraction dissociation of a virtual photon on a dipole of transverse size r_0 . Using the hypothesis formulated in [1] (i.e. assuming that the nucleon is a collection of a number (n_{eff}) of QCD dipoles) we estimated the relevant cross-sections on the nucleon target. Our conclusions can be formulated as follows.

- (a) Measurements of the forward differential diffractive cross-section shall provide a significant test of the applicability of the Good-Walker idea [10] on the origin of diffraction dissociation.
- (b) Fairly precise predictions can be made for the longitudinal quasi-elastic contribution. The results for other components are somewhat ambiguous. The transverse quasi-elastic component is sensitive to the non-perturbative region of large transverse sizes in the photon wave function (corresponding to the "aligned jets" of Ref.[31]) and therefore depends on additional non-perturbative parameters. Its measurements may thus provide an interesting information on non-perturbative physics at small

⁴This observation is consistent with the measurements of rapidity distribution of particles produced in high-energy hadronic collisions and of "stopping power" in hadron-nucleus collisions [33].

 $x_{\rm Bj}$. There is thus a strong interest in separate measurements of longitudinal and transverse components of the diffractive structure functions. The 3-Pomeron component is sensitive to the probability of gluon emission at large rapidity and thus to the effects of energy-momentum conservation which are neglected in the QCD dipole model (and in the whole BFKL approach).

- (c) Within the ambiguities listed above, the obtained structure functions turn out to be of the same order as those obtained from a simple extrapolation of the existing data [30] to $p_t = 0$. The detailed comparison with the future precise data shall thus be very illuminating.
- (d) The obtained effective pomeron intercept (including logarithmic corrections) turns out to be close to that measured in F_2 , i.e., in the total γ^* cross-section (and even somewhat larger in the 3-Pomeron region). Thus we predict a substantially stronger x_P dependence of diffractive structure functions at $p_t = 0$ than that observed till now at larger p_t [9, 16, 17, 29].
- (e) Our calculation predicts a rich structure of the scaling violation. Longitudinal quasielastic component is expected to decrease with increasing Q^2 . The transverse one increases to a limiting value at large Q^2 . The 3-Pomeron contribution increases, following approximately a power law in Q^2 .

To summarize, the QCD dipole picture predicts some interesting physics to be found in the diffractive structure functions at $p_t = 0$. It remains to be seen if this shall indeed show up in the future measurements.

Several comments are in order.

(i) The forward elastic dipole-dipole amplitude given by (3) is the integral of the amplitude at a fixed impact parameter:

$$T(r; p_t = 0) = \int d^2b T(r; b)$$
. (50)

The numerical MC estimates reported in [34] indicate that T(r; b) violates unitarity at small impact parameters. This was shown in [34] not to be essential for the value of the integrated amplitude $T(r; p_t = 0)$

- given in (50), at least at the presently available energies. Therefore we expect that also in our case the possible violation of unitarity should not invalidate the obtained estimates.
- (ii) It was shown in [4] that the diffractive cross-section calculated at fixed p_t in the 3-Pomeron region, when extrapolated to $p_t = 0$, reveals a singularity of the form $\sim p_t^{-1}$. Our calculation shows explicitly how this singularity is regularized by the energy-dependent cut-off in impact-parameter space [5]

$$\log^2 b^2 / r_0^2 \le 2[a(x_{\rm Bj})]^{-1} \equiv \frac{14\alpha N_c \zeta(3) \log(1/x_{\rm Bj})}{\pi}.$$
 (51)

- (iii) The leading logarithmic approximation which is at the origin of the BFKL approach (and thus also of the QCD dipole picture) does not allow to fix uniquely the energy scale. Therefore relation of the variables $x_{\rm Bj}$ and x_P to Y and y is somewhat arbitrary. This is particularly controversial in the case of the quasi-elastic component, where the dipole picture suggests Y as the relevant variable, whereas the experience from Regge phenomenology suggests y instead [17]. We have taken Y to be fully consistent in our derivation of Eq. (6) (if y is taken, (9) is inconsistent with (6)).
- (iv) It was suggested in [14] that rapidity variable Y can be affected by the value of the light-cone momentum fraction η in the photon wave function, e.g.,

$$Y = \log\left(\frac{c\eta(1-\eta)}{x_{\rm Bj}}\right). \tag{52}$$

In the present paper we have taken the conservative approach and neglected this possibility. It is interesting to note, however, that this effect would strongly reduce the contribution from the regions $\eta \approx 0$ and $\eta \approx 1$. Consequently, the sensitivity of the calculations to the non-perturbative contributions would be substantially reduced.

We would like to thank D. Kisielewska, A. Eskreys and R. Peschanski for discussions.

References

- [1] H. Navelet, R. Peschanski, Ch. Royon, *Phys. Lett.* **B366**, 329 (1995).
- [2] H. Navelet, R. Peschanski, Ch. Royon, S. Wallon, Phys. Lett. B385, 357 (1996).
- [3] A.H. Mueller, Nucl. Phys. **B415**, 373 (1994).
- [4] A.H. Mueller, B. Patel, Nucl. Phys. **B425**, 471 (1994).
- [5] A.H. Mueller, Nucl. Phys. **B437**, 107 (1995).
- ZEUS coll., M. Derrick et al., Phys. Lett. B316, 201 (1993); H1 coll., I.
 Abt et al., Nucl. Phys. B407, 515 (1993); Phys. Lett. B321, 161 (1994).
- [7] L.N. Lipatov, Sov. J. Nucl. Phys. 23, 642 (1976); V.S. Fadin, E.A. Kuraev, L.N. Lipatov, Phys. Lett. B60, 50 (1975); E.A. Kuraev, L.N. Lipatov, V.S. Fadin, Sov. Phys. JETP 44, 45 (1976), 45, 199 (1977);
 I.I. Balitsky, L.N. Lipatov, Sov. J. Nucl. Phys. 28, 822 (1978).
- [8] See, e.g., A. Donnachie, P.V. Landshoff, Acta Phys. Pol. B27, 1767 (1996);
 J.R. Cudell, A. Donnachie, P.V. Landshoff, Nucl. Phys. B482, 241 (1996);
 I. Bojak, M. Ernst, Nucl. Phys. B508, 731 (1997) and references quoted there.
- [9] H1 Coll. T. Ahmed et al., Phys. Lett. B348, 681 (1995); ZEUS Coll. M. Derrick et al., Z. Phys. C68, 569 (1995).
- [10] M.L. Good, W.D. Walker, *Phys. Rev.* **120**, 1857 (1960).
- [11] A. Eskreys, private communication.
- [12] J. Bartels, Phys. Lett. B298, 204 (1993); Z. Phys. C62, 425 (1994); J. Bartels, M. Wuesthoff, Z. Phys. C66, 157 (1995).
- [13] A. Bialas, W. Czyz, Acta Phys. Pol. B29, 651 (1998); A. Bialas, W. Czyz, W. Florkowski, Phys. Rev. D55, 6830 (1997).
- [14] A. Bialas, Acta Phys. Pol. **B28**, 1239 (1997).

- [15] For a review, see H. Lotter, Thesis, DESY 96-262 (1996).
- [16] A. Bialas, R. Peschanski, *Phys. Lett.* **B378**, 302 (1996).
- [17] A. Bialas, R. Peschanski, *Phys. Lett.* **B387**, 405 (1996).
- [18] N.N. Nikolaev, B.G. Zakharov, Z. Phys. C64, 631 (1994).
- [19] M. Genovese, N.N. Nikolaev, B.G. Zakharov, Zh. Eksp. Teor. Fiz. 108, 1141, 1155 (1995).
- [20] L. Stodolsky, Phys. Rev. Lett. 18, 135 (1967).
- [21] K. Gottfried, D.R. Yennie, Phys. Rev. 182, 1595 (1969).
- [22] S. Brodsky, L. Frankfurt, J.F. Gunion, A.H. Mueller, M. Strikman, *Phys. Rev.* **D50**, 3134 (1994).
- [23] L. Frankfurt, W. Koepf, M. Strikman, Phys. Rev. **D54**, 3194 (1996).
- [24] See e.g. A. Kaidalov, Phys. Rep. 50, 157 (1979).
- [25] J.D. Bjorken, J. Kogut, D. Soper, Phys. Rev. **D3**, 1382 (1971).
- [26] P.S. Gradstein, I.M. Rhyzhik, *Tablitsy integralov, sum, riadov i proizvedenii*, Moscow 1971, 5th ed., p.707.
- [27] M. Abramovitz, I.A. Stegun, *Handbook of Mathematical Functions*, Dover, N. Y.,p.559.
- [28] J.D. Bjorken, SLAC-PUB-7096 (1966).
- [29] A. Bialas, Acta Phys. Pol. **B27**, 1263 (1996).
- [30] ZEUS coll., J. Breitweg et al., DESY preprint 97-184 (1997).
- [31] J.D. Bjorken, J. Kogut, Phys. Rev. D8, 1341 (1973).
- [32] B. Andersson, Acta Phys. Pol. **B29**, 1885 (1998).
- [33] See, e.g., W. Busza, A. Goldhaber, *Phys. Lett.* **B139**, 235 (1984).
- [34] G.P. Salam, Nucl. Phys. **B461**, 512 (1996).

This figure "fig1-1.png" is available in "png" format from:

http://arxiv.org/ps/hep-ph/9808437v1

This figure "fig1-2.png" is available in "png" format from:

http://arxiv.org/ps/hep-ph/9808437v1